Separation Science and Technology
Publication details, including instructions for authors and subscription information:
http://www.informaworld.com/smpp/title~content=t713708471

Hydrophobic pervaporation: influence of the support layer of composite membranes on the mass transfer

F. Lipnizki[a]; J. Olsson[a]; P. Wu[b]; A. Weis[c]; G. Trägårdh[a]; R. W. Field[b]
[a] Lund University, Lund, Sweden [b] Department of Chemical Engineering, University of Bath, Bath, UK [c] Universität Bonn, Bonn, Germany

Online publication date: 29 May 2002

To cite this Article Lipnizki, F. , Olsson, J. , Wu, P. , Weis, A. , Trägårdh, G. and Field, R. W.(2002) 'Hydrophobic pervaporation: influence of the support layer of composite membranes on the mass transfer', Separation Science and Technology, 37: 8, 1747 — 1770
To link to this Article: DOI: 10.1081/SS-120003042
URL: http://dx.doi.org/10.1081/SS-120003042

SEPARATION SCIENCE AND TECHNOLOGY, 37(8), 1747–1770 (2002)

HYDROPHOBIC PERVAPORATION: INFLUENCE OF THE SUPPORT LAYER OF COMPOSITE MEMBRANES ON THE MASS TRANSFER

F. Lipnizki,[1] J. Olsson,[1] P. Wu,[2] A. Weis,[3] G. Trägårdh,[1,*] and R. W. Field[2]

[1]Food Engineering, Lund University, P.O. Box 124, SE-221 00 Lund, Sweden
[2]Department of Chemical Engineering, University of Bath, Bath BA2 7AY, UK
[3]Institut für Lebensmitteltechnologie, Universität Bonn, D-53117 Bonn, Germany

ABSTRACT

The opportunities of using hydrophobic pervaporation to concentrate organic components in aroma recovery and wastewater treatment have been recognized widely. The focus of this article is on the influence of the support layer on the mass transfer in hydrophobic pervaporation. Even though the influence of the support layer on the overall mass transfer has been observed experimentally, the modeling and analysis of this aspect has been widely neglected. The aim of this study is to build a bridge between modeling of the influence of the support layer and experimental data. Therefore, an improved modeling approach is proposed and used to analyze experimental data for the

*Corresponding author.

permeation of the two binary systems water–phenol and water–chloroform through hydrophobic composite polydimetylsiloxane membranes. Comparing the experimental results with the model, it has been observed that the mass transfer of the support layer depends on both physical and chemical properties of the support layer. On the basis of these observations, guidelines for the selection of support layers will be presented.

Key Words: Pervaporation; Hydrophobic membrane; Modeling; Support layer

INTRODUCTION

Even though the industrial applications of hydrophobic pervaporation only started recently, the opportunities of using hydrophobic pervaporation to concentrate organic components from aqueous solutions has been widely recognized in aroma recovery and waste-water treatment. To strengthen the market position of pervaporation, further improvements on the membrane performance are required. While present research mainly focus on the development of new membrane polymers combining high selectivities and fluxes, this study is dealing with one of the widely neglected aspects of membrane design, the influence of the support structure on the mass transfer through composite membranes. Even though the development of homogenous membranes for pervaporation is desirable, e.g., from a manufacturing point of view, most of the membranes tested and applied in pervaporation so far are composite membranes, consisting of a selective layer and a support layer. While the thin selective layer should generally provide the selectivity of the membrane and determine the fluxes, the support layer should give the membrane its mechanical stability. However, the nature of the support layer can also influence the mass transfer through the composite membrane and in some cases it even dominates and reverses the performance of the selective layer. The number of studies on the influence of the support on the performance of pervaporation is relatively small. The focus of this study is therefore on the influence of the support layer on the mass transfer in hydrophobic pervaporation. After reviewing previous studies on the influence of the support layer in hydrophobic pervaporation, an improved model will be presented based on the solution-diffusion model. This modeling approach covers the influence of the interface layer and the porosity of the support layer on the diffusion path through the selective layer as well as the effect of the pressure drop in the support layer on the driving force. This model will then be discussed by analyzing permeabilities of the binary feed solutions of phenol–water and chloroform–water through

polydimetylsiloxane (PDMS) membranes with different support layers. Furthermore, experimental data previously published by Börjesson et al. (l)for recovery of low concentrations of aroma components from aqueous solutions will be considered in the discussion. The implications for the selection of support layers will be discussed and recommendations for the selection of the support layer materials will be given.

MODELING OF THE SUPPORT LAYER IN HYDROPHOBIC PERVAPORATION

While in hydrophilic pervaporation, some researchers (2–9) have previously studied and modeled the effect of the support layer of composite membranes, this aspect has been neglected widely in hydrophobic pervaporation. This might be due to the fact that it appears that for some systems the support layer does not affect the mass transfer and seems therefore to be negligible. Nijhuis (10) studied the removal of toluene from water using polyoctenamer membrane without a support and with a polysulfone support, while Stürken (11) analyzed the separation of 1,2 dichloroethane and water using a PDMS membrane with poly(vinylidene fluoride) (PVDF) and poly(ether imide) (PEI) support. In both cases the influence of the support was found to be negligible.

Nevertheless, other researchers observed the effect of the support layer in hydrophobic pervaporation without modeling. Scholz et al. (12) tested zeolite-filled silicone membranes with different support materials for the removal of ethanol from water. It was observed that both flux and selectivity changed with the support. From their experimental studies it was concluded, that in order to achieve high selectivities combined with high fluxes high porous support structures are required. Furthermore, using different etched support layers, it was observed that too large pores can lead to large interface layer due to plugging of the pores with a reduction in flux. Further, in case of large pore diameter the selective top layer tends to be less tight and the risk of leakage increases. This was also highlighted in a general study by Heinzelmann (13) who discussed the relationship between the support of composite membranes and coating of selective layer on the performance of pervaporation membranes. Rautenbach and Klatt (14) showed the importance of the support layer for the removal of phenol from water using a hydrophobic polybutadiene membrane on polyhydantoine supports with different porosities. In accordance to previous studies it was observed that the composite membrane with the lower support layer porosity had a significantly lower total flux and selectivity. Borges et al. (15) tested five different composite membranes with an ethene–propene–diene rubber (EPDM) top layer and different porous PEI hollow fibres as support structures for the recovery of trichloroethylene and dichloromethane from water. A strong

influence of the support layer on the overall mass-transfer coefficient was observed and was related to different surface porosities of the support layer and the length of the intrusion depth into the support layer. It was noted that a low-surface porosity of the support lead to high resistance for the organic component, while the water flux was independent of the support. In a study by Feng and Huang (16) selectivities and fluxes of a homogeneous PDMS membrane, a symmetric silicone–polycarbonate co-polymer membrane, and an ultrathin silicone membrane with a microporous support were tested for the separation of an isopropanol–water mixture. It was observed that both the homogeneous PDMS membrane and the symmetric silicone–polycarbonate co-polymer membrane were isopropanol selective, while the silicone–polycarbonate co-polymer membrane on a microporous support was slightly water selective. It was assumed that the relatively tight porous support was produced from a water selective plastic and therefore changed the selectivity of the overall membrane. Most recently Vankelecom et al. (17) studied the effect of intrusion of PDMS in Zirfon® (*polysulfone filled zirconium oxide*) support layers for the system water–ethanol. Applying different pre-treatments of the support layer, it was observed that the normalized fluxes of the composite membrane changed, while the selectivity remained the same. It was further noted that independent of the pre-treatment it was not possible to stop the PDMS from intruding the support.

Combining previous models in a new approach, the modeling of the influence of support layer in hydrophobic pervaporation can be divided into three sections. The first section is focusing on the influence of the support layer on the diffusion path ("Influence of Support Layer on the Diffusion Path"), the second section on the driving force ("Pressure Loss in the Support Layer") and the final section on the influence of permeate condensation in the pores ("Permeate Condensation in the Pores").

Influence of Support Layer on the Diffusion Path

The top layer and the support layer of composite membranes are generally connected by an interface layer, see Fig. 1. This interface layer is a result of the two-step manufacturing process of composite membranes:

1. production of the porous support layer, commonly commercial micro- or ultrafiltration membranes are used, and
2. deposition of the selective layer on the surface of the support layer.

Due to deposition of the selective layer onto the support layer it might be unavoidable that pores are partly filled with the selective polymer as reported by Vankelecom et al.(17). This intrusion into the support layer leads to the interface

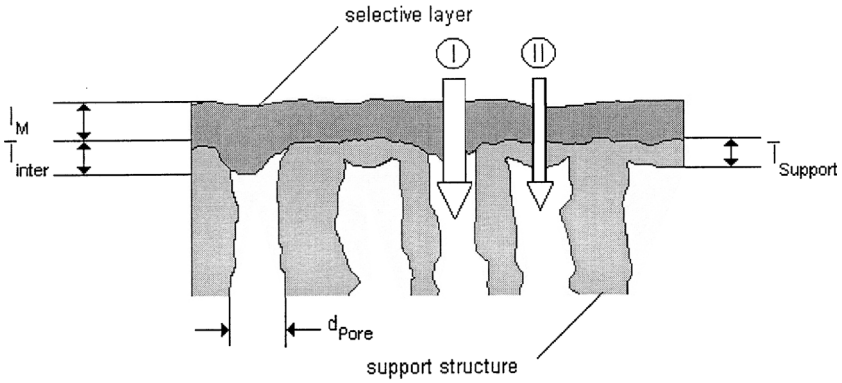

Figure 1. Schematic drawing of the interface layer.

layer, which can be observed as a result of all common preparation techniques of composite membranes, e.g., separate casting, direct coating, gas phase deposition, and interfacial polymerization.

In gas separation the resistance of the interface layer is either described by two resistances in parallel approach (18,19) or by one overall resistance, which effectively combines the two resistances (20). The resistance approach divides the flux through the interface layer into a flux through the support layer material and a flux through the selective polymer filled pores. Gudernatsch et al. (21,22) adopted this approach for hydrophobic/hydrophilic pervaporation. Referring to Fig. 1 it has been assumed that there are two different mass transport paths with different resistances through a composite membrane:

Path I : selective layer $\Rightarrow$ interface layer $\Rightarrow$ pores of support

Path II : selective layer $\Rightarrow$ support material $\Rightarrow$ pores of support.

With regard to possible mass-transfer paths through the membrane, Koops (3) noted that generally the whole support layer including pore walls could be used for the mass transfer. However, generally only the two paths shown in Fig. 1 will be used since they offer the lowest resistance. On the basis of this, the flux through the membrane can be described by:

$$J_i = \left(\frac{1}{\mathscr{R}_{\text{Path I}}} + \frac{1}{\mathscr{R}_{Path\,\text{II}}}\right)(a_{i,\text{F}} - a_{i,\text{P}}) \tag{1}$$

The membrane porosity of the support layer can be expressed by:

$$\epsilon_{\text{S}} = \frac{A_{\text{Pore}}}{A_{\text{M}}} \tag{2}$$

An approach to estimate the average pore length filled with selective polymer is to assume that the filling has a round shape with a radius of approximately $d_{\text{pore}}/2$ due to the production process. On the basis of this assumption the average thickness of the interface layer is:

$$\bar{l}_{\text{Inter}} = \frac{1}{3} d_{\text{Pore}} \tag{3}$$

It was further assumed that the thickness of the skin layer of the support layer used for mass transport is similar to the thickness of the interface layer:

$$\bar{l}_{\text{Support}} = \bar{l}_{\text{Inter}} \tag{4}$$

Both assumptions have been confirmed by scanning electron microscope (SEM) pictures taken of all the membranes considered in this study (see "Feed Solution"). Hence, similar to Gudernatsch et al. (21,22) Eq. (1) can be rewritten as:

$$J_i = \left(\frac{\epsilon_S}{\frac{l_M + \bar{l}_{\text{Inter}}}{P_{i,M}}} + \frac{(1 - \epsilon_S)}{\frac{l_M}{P_{i,M}} + \frac{\bar{l}_{\text{Support}}}{P_{i,\text{Support}}}} \right) (a_{i,F} - a_{i,P}) \tag{5}$$

Hence, flux is a function of the geometrical characteristics of the porous support structure, given by the surface porosity and thickness of the support structure. The applicability of the approach was demonstrated by Gudernatsch et al. (21,22) for the recovery of ethanol from water using a hydrophobic PDMS membrane on a more hydrophilic polysulfone support. In this study, the porosity of the support has been varied and the separation characteristics of membrane have been changed from hydrophilic at low porosities of the support to hydrophobic at high porosities (21,22). In a later study Bai et al. (23) reported a similar effect of the support material on the flux and selectivity for PDMS membranes with a more hydrophilic PEI support for the recovery of acetic acid from water. By changing the porosity of the support it was possible to shift the membrane selectivity from water selective to acetic acid selective.

On the basis of Eq. (5) two different boundary cases can be distinguished. In the first case the mass transport is dominated by the transport through Path I ($P_{i,M} \gg P_{i,\text{Support}}$). Therefore, Eq. (5) can be reduced to:

$$J_i = \left(\frac{\epsilon_S P_{i,M}}{l_M + \bar{l}_{\text{Inter}}} \right) (a_{i,F} - a_{i,P}) \tag{6}$$

In the second case the mass transport will be determined by Path II ($P_{i,\mathrm{M}} \approx P_{i,\mathrm{Support}}$). In this case the flux can be described by:

$$J_i = \left(\frac{P_{i,\mathrm{M}}}{l_{\mathrm{M}} + \bar{l}_{\mathrm{Inter}}}\right)(a_{i,\mathrm{F}} - a_{i,\mathrm{P}}) \tag{7}$$

On the basis of the previous approaches by Gudernatsch et al. (21,22) a new modeling approach is suggested in this study. This approach takes the nature of the support material into account. Generally two types of hydrophobic composite membranes can be distinguished:

1. composite membranes with a hydrophilic support e.g., PEI, poly(ether sulfone) (PES), and
2. composite membranes with a hydrophobic support e.g., PVDF, polyproplyene (PP).

It should be noted that polyacrylonitrile (PAN), one of the most common supports in pervaporation, is generally expected to be strongly hydrophilic but in practice it has been observed to be hydrophobic; the same has been observed for the hydrophobic PVDF, which can become hydrophilic through an appropriate surface treatment (24).

Combining the geometry of the membrane with physicochemical interactions between permeating components and support layer, the flow through a composite membrane can be determined using the equations given in Table 1.

Pressure Loss in the Support Layer

The mass transport of permeate through the porous support layer is based on convective flow. Hence a pressure gradient can be observed between the interface layer and the permeate channel, which can influence the driving force of the mass transport:

$$J_i = \frac{P_{i,\mathrm{M}}}{l_{\mathrm{M}}}\left(a_{i,\mathrm{F}} - y_i\varphi_i\frac{p_{\mathrm{P}} + \Delta p}{p_i^{\mathrm{Sat}}}\right) \tag{8}$$

The pressure drop depends on the mass transport through the porous structure. An approach to estimate the influence of this effect is the capillary model. In this model the porous structure is assumed to consist of similar sized and parallel capillaries. Depending on the pore diameter and the mean free path of the permeate, two different types of flow through these capillaries can be distinguished:

- viscous flow, which is dominated by gas–gas molecule collisions, and
- molecular or Knudsen flow, which refers to collisions between the pore walls and the gas molecules.

Table 1. Flux Equations for Different Support Layers and Permeating Components

Case I: $P_{w,M} \gg P_{w,support}$ and $P_{o,M} \approx P_{o,support}$		
Flux of water	$J_w = \left(\frac{\epsilon_s P_{w,M}}{l_M + \bar{l}_{Inter}}\right)(a_{w,F} - a_{w,P})$	(15)
Flux of organic component	$J_o = \left(\frac{P_{o,M}}{l_M + \bar{l}_{Inter}}\right)(a_{o,F} - a_{o,P})$	(16)
Case II: $P_{w,M} \approx P_{w,support}$ and $P_{o,M} \approx P_{o,support}$		
Flux of water	$J_w = \left(\frac{\epsilon_s}{\frac{l_M + \bar{l}_{Inter}}{P_{w,M}}} + \frac{(1-\epsilon_s)}{\frac{l_M}{P_{w,M}} + \frac{\bar{l}_{Support}}{P_{w,Support}}}\right)(a_{w,F} - a_{w,P})$	(17)
Flux of organic component	$J_o = \left(\frac{\epsilon_s}{\frac{l_M + \bar{l}_{Inter}}{P_{o,M}}} + \frac{(1-\epsilon_s)}{\frac{l_M}{P_{o,M}} + \frac{\bar{l}_{Support}}{P_{o,Support}}}\right)(a_{o,F} - a_{o,P})$	(18)
Case III: $P_{w,M} \approx P_{w,support}$ and $P_{o,M} \gg P_{o,support}$		
Flux of water	$J_w = \left(\frac{P_{w,M}}{l_M + \bar{l}_{Inter}}\right)(a_{w,F} - a_{w,P})$	(19)
Flux of organic component	$J_o = \left(\frac{\epsilon_s P_{o,M}}{l_M + \bar{l}_{Inter}}\right)(a_{o,F} - a_{o,P})$	(20)

The Knudsen number Kn (the ratio of the mean free path length λ, over the capillary radius $d_{\text{Pore}}/2$) can be used to evaluate the flow through the capillaries:

$$Kn = \frac{2\lambda}{d_{\text{Pore}}} \tag{9}$$

The required mean free path is the average distance traversed by molecules between collisions and can be estimated, using the component values of the permeate by (25):

$$\lambda = 32\frac{\eta_{\text{P}}}{p_{\text{P}}}\left(\frac{RT}{2\pi M_{\text{P}}}\right)^{1/2} \tag{10}$$

In the case of viscous flow ($Kn < 10^{-2}$) the pressure drop for an ideal gas can be estimated by (26):

$$\Delta p = \frac{32 J_{\text{Total}}\tau l_{\text{Pore}}\eta_{\text{P}}RT}{\epsilon d_{\text{Pore}}^2 p_{\text{P}}^{\text{av}}} \tag{11}$$

In the case of Knudsen flow or molecular flow, ($Kn > 10$) the pressure drop for an ideal gas can be determined by (26):

$$\Delta p = \frac{3 J_{\text{Total}} l_{\text{Pore}}\tau\sqrt{RTM_{\text{P}}}}{2^{3/2} d_{\text{Pore}}\epsilon} \tag{12}$$

The problem in both cases is that the pressure drop depends on the total flux J_{Total} through the membrane. Since the flux through the membrane and the pressure drop are linked, the influence of the pressure drop can only be determined by iteration or by independent gas permeation experiments with the support structure, e.g., Beuscher and Gooding (27) applied the dusty gas model to predict permeation of binary gas mixtures after experimentally determining the morphological parameters of the support. Overall, the influence of the pressure drop in the support layer on the mass transport will be mainly determined by the total flux, the pore diameter, and the sensitivity of the permeating component towards pressure changes. Hence, in case of membranes with very mall pores and pressure-sensitive components with a low-equilibrium vapor pressure, this effect might influence the mass transport significantly. In this study with asymmetric support structure it can be assumed that in the area with small pores, directly below, the selective layer Knudsen flow occurs, while in the areas with more open pores molecular flow is expected.

Permeate Condensation in the Pores

The effect of condensation in the support layer has been first discussed by Albrecht (28) and Rautenbach and Albrecht (29) for the dehydration of isopropanol using asymmetric cellulose triacetate membranes. In the study the possibility of pore condensation was highlighted and the following relation was proposed to calculate the pressure at which pore condensation occurs:

$$p_i^{\mathrm{C}} = p_i^{\mathrm{Sat}} \exp\left(-\frac{4\sigma \tilde{V}_i}{d_{\mathrm{Pore}} RT}\right) \tag{13}$$

On the basis of theoretical modeling and experiments it was suggested, that the support structure should have finger typed pores with large diameters (28,29). On the other hand the pore diameters should not be too large, since problems in achieving a defect-free top layer might occur (3). Even though this study was originally based on asymmetric hydrophilic membranes, it is also relevant to hydrophobic composite membranes, since most support layers are asymmetric membranes and pore condensation depends only on the structure of the support and not on its chemical nature. Consequently, the pore condensation is also important in the design of composite membranes for hydrophobic applications. Similar to the pressure loss in the support layer, this effect becomes increasingly important for membranes with small pore diameters and pressure-sensitive components with a low-equilibrium vapor pressure.

MATERIALS AND METHODS

Feed Solution

Two binary systems water–phenol and water–chloroform were selected for this study. Phenol (C_6H_6O) with a boiling point of 181.75°C (at 1.013 bar) has a low-equilibrium vapor pressure. Its concentration in the feed solution was set to be 2 wt.%. Since phenol is a weak acid, the pH-value might influence the membrane performance and the analysis, it was therefore adjusted to 7 for all experiments.

Chloroform or trichloromethane ($CHCl_3$) has a boiling point of 61.3°C (at 1.013 bar) and has a high-equilibrium vapor pressure. The feed concentration of chloroform was set to 0.3 wt.%. However, to account for the effect of evaporation of chloroform, a freshly prepared feed solution was used for each experiment and monitored by taking stitch samples from the feed.

At their feed temperatures both components are fully dissolved in water. The water used as the solvent was distilled and the purity of the organic components used to prepare the feed solution was 99.5% in both cases.

Pervaporation Membranes

In this study four different membranes with a PDMS toplayer manufactured by GKSS Forschungszentrum (Geesthacht, Germany) were investigated. The support materials of three of these membranes were PVDF, PAN, and PEI with a selective layer thickness of 1 μm. A membrane with PVDF support and a 5 μm selective layer was also tested. The structure of these membranes was analyzed using a SEM JEOL 6310 (Jeol Ltd., Akishima, Japan). Before the analysis, the samples of the membranes were dipped into liquid nitrogen and then cut with a razor. After this, the samples were coated with gold using a sputter coater 150B (Edwards, Crawley, W. Sussex, UK). Even though it was impossible to obtain accurate measurements of membrane structure, i.e., the porosity and pore size diameter of the support layer, the following order of pore size diameters in the support could be obtained from the SEM-pictures:

PVDF $>$ PEI $>$ PAN

The SEM pictures of the membranes are shown in Fig. 2 and give an impression of how the structure of the support varies with the support material.

Pervaporation Apparatus

The layout of the experimental set-up and the test-cell are shown in Fig. 3. The membrane area of the stainless steel pervaporation test cell was 22.9 cm^2 and the volume of the feed tank was 500 cm^3.

The membranes were clamped into the test cell on a porous sintered metal support and sealed with two "o"-rings. The test cell was placed on a hotplate, which also controlled the magnetic stirrer. The temperature in the feed tank was controlled by a thermocouple connected to an electronic control system. On the permeate side the vacuum was maintained by a vacuum pump. The permeate was collected and condensed in cold traps using liquid nitrogen. To avoid condensation in the permeate channel between the test cell and the cold trap, additional heating of the permeate outlet was provided using an electric trace heating.

Experimental Procedures

The feed temperature was set to be 70°C for phenol and 25°C for chloroform and kept constant during the experiments. To reduce the effect of concentration polarization, the magnetic stirrer in the feed tank was adjusted to 1000 rpm to have a turbulent flow regime ($Re > 100{,}000$) in the tank. After the

feed temperature was reached, the nitrogen container of the cold trap was filled and the vacuum pump was switched on. During the experiments the permeate side pressure was maintained below 2 mbar. The permeate was collected during a measured length of time and then weighed and analyzed to determine flux and selectivity. Each set of experiments was repeated at least three times until constant results with deviation of $\pm 10\%$ or less were obtained in three consecutive experiments.

Analysis

The total flux was measured gravimetrically using a microbalance (Mettler Instruments AG, Greifensee-Zürich, Switzerland) by weighting the cold trap before and after the experiments with an error of 0.05%.

In case of phenol both feed and permeate were sampled and analyzed for concentrations using a Cecil 1020 UV-spectrometer (Cecil Instruments Ltd., Cambridge, UK). The UV-spectrometer was calibrated using a series of standard solutions between 25 and 100 ppm. A linear relationship between spectrometer adsorbance reading and the sample concentration was observed for phenol concentrations up to 100 ppm. For this range, it was therefore assumed that the Lambert–Beer Law is valid. To use this linear relationship between adsorption and concentration, the samples were diluted to concentrations between 30 and 100 ppm with distilled water. The final concentrations were calculated taking this dilution into account. Further, since the ambient temperature can effect the spectrometer adsorbance reading, calibration was conducted before every analysis.

Due to the low solubility of chloroform in water, phase separation occurred in the permeate. To obtain a homogeneous phase for analysis, the permeate was diluted with a measured quantity of 2-propanol. In case of chloroform, both feed and permeate streams were analyzed using a Mettler D18 Karl Fischer titrator (Mettler-Toledo Inc., Columbus, OH) and standard solvents (BDH Laboratory Supplies, Poole, Dorset, UK) to determine the water concentration. Further each batch of 2-propanol itself can adsorb water and was therefore analyzed for it. The water content of the 2-propanol was subtracted from the total water mass found in the permeate/2-propanol solution to determine the water concentration of the permeate.

Estimation of the Permeability

In order to compare the different membrane and support structures the permeability as transport flux per unit driving force was selected as standard.

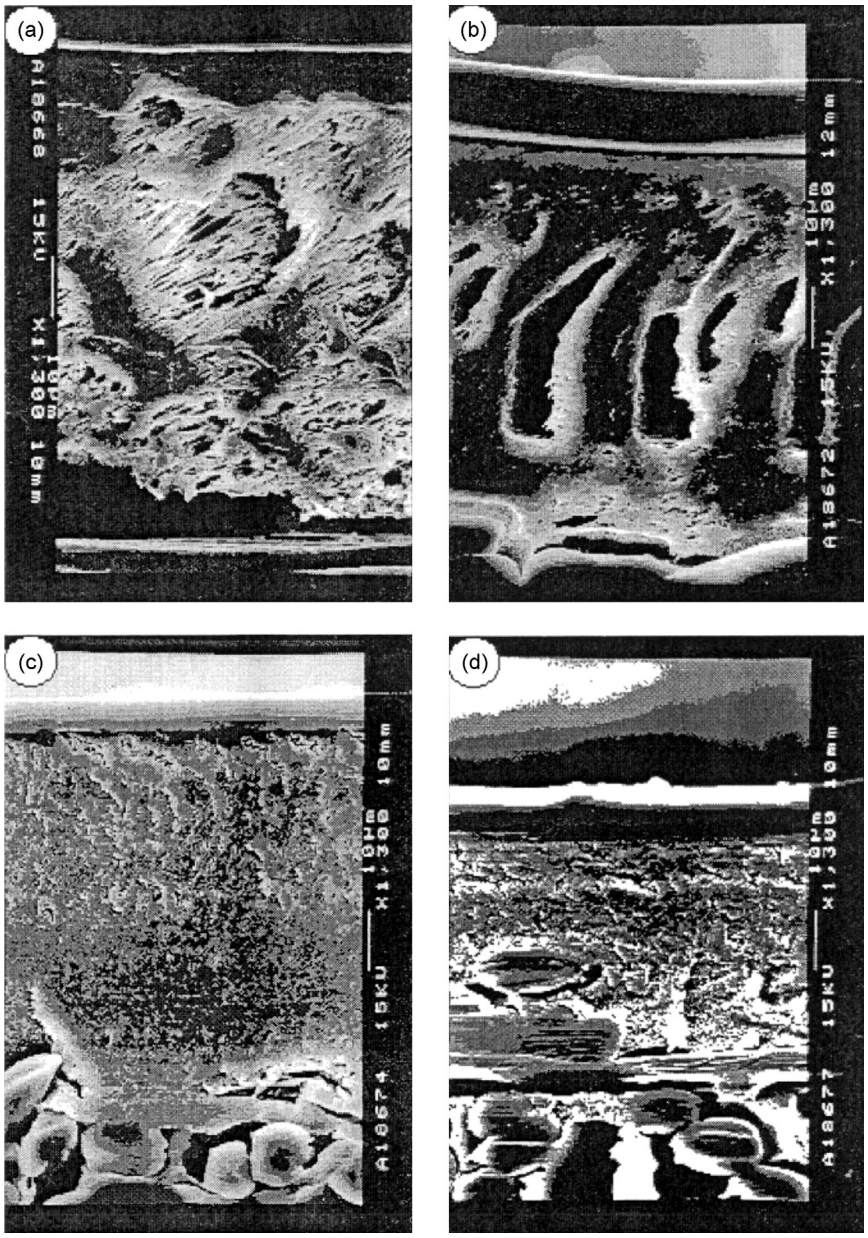

Figure 2. SEM photographs of the different PDMS Membranes from GKSS Forschungszentrum used in this study at 1300 × magnification. (a) PDMS (1 μm) with PVDF support, (b) PDMS (5 μm) with PVDF support, (c) PDMS (1 μm) with PEI support, and (d) PDMS (1 μm) with PAN support.

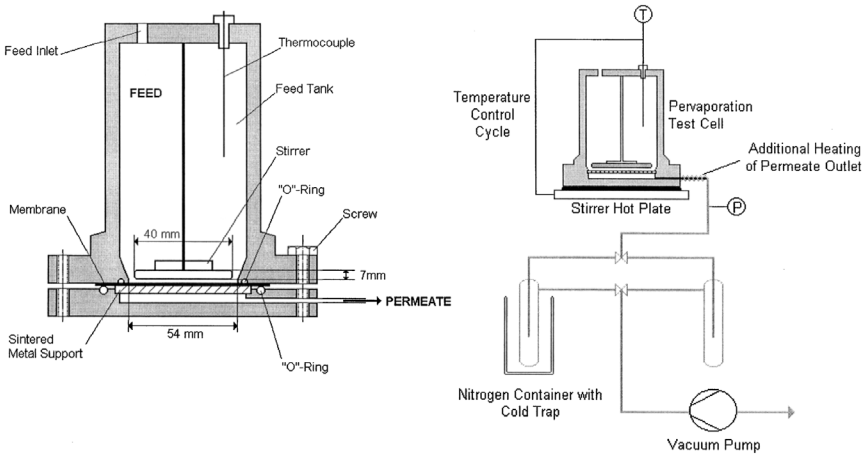

Figure 3. Left, test cell and right, experimental set-up.

Assuming the influence of the permeate side concentration boundary layer is negligible, the permeability can be determined based on the overall mass transfer by (30,31):

$$P_i = \frac{l_M}{\frac{(a_{i,F}-a_{i,P})}{J_i} - \frac{\gamma_{i,F}}{k_{Bo,i}\rho_M^{Av}}} = \frac{l_M}{\frac{\left(x_{i,F}\gamma_{i,F} - y_{i,P}\varphi_i\frac{p_P}{p_i^{Sat}}\right)}{J_i} - \frac{\gamma_{i,F}}{k_{Bo,i}\rho_M^{Av}}} \tag{14}$$

The feed side activity coefficients of phenol and chloroform required in Eq. (14) were estimated using the modified UNIFAC method based on a software packet (DDBST Software & Separation Technology, Oldenburg, Germany). Due to the low concentrations of the organic components in the feed, the activity coefficients were determined at infinite dilution accounting for the feed temperature. The activity coefficient of phenol was determined to be 28.85 and of chloroform to be 658.3. The activity on the permeate side has been assumed to be negligible, due to the low permeate pressures of less than 2 mbar.

Further, the mass-transfer coefficients through the concentration boundary layer for phenol and chloroform are required to determine the permeability. Bennett (32) using the experimental apparatus described above, observed that the effect of concentration polarization for the system phenol–water with a PDMS membrane at a feed temperature of 70°C and a stirrer speed greater than 250 rpm ($Re > 25{,}000$) is negligible. Since the stirrer speed in this study is 1000 rpm ($Re > 100{,}000$), this assumption should also be valid for this study and the term accounting for the mass-transfer coefficient through the concentration boundary layer can be discarded in Eq. (14). In the same study

Bennett (32) also analyzed the system chloroform–water with a PDMS membrane at a feed temperature of 25°C. Even at a stirrer speed of 1000 rpm the influence of concentration polarization was significant. The mass-transfer resistance of the concentration boundary for chloroform $k_{\mathrm{Bo,chloroform}}$ was determined to be 4.765×10^{-5} m/sec at a feed temperature of 25°C and a stirrer speed of 1000 rpm. Hence, the concentration boundary layer was considered in the calculation of the chloroform permeability. The assumption that the concentration boundary layer is more important for chloroform than for phenol has been further confirmed by using the Sherwood correlation for stirred cells by Smith et al. (33) assuming geometrical similarity between the stirred cells and using the Wilke–Chang method (34) to estimate the diffusion coefficients of the organic components at infinite dilution.

RESULTS AND DISCUSSION

In Table 2 the results for the two systems phenol–water and chloroform–water analyzed in this study are presented. It is apparent that the fluxes and selectivities for the different types of PDMS-membranes vary significantly with membrane thickness and support layer. The changes of flux and selectivity with membrane thickness are shown in Table 2 and are a well-known and studied phenomena. Generally, with an increasing membranes thickness,

(1) the fluxes of the permeating components are reduced, and
(2) the selectivity of the membrane is increased.

These trends can also be observed for the membranes in this study. More interesting are the change of fluxes and selectivities with the support layer material.

Focusing first on the fluxes of the components (Table 2), it can be found that the water fluxes through membranes with a hydrophilic PEI-support are always the highest fluxes, while membranes with PAN-support reveal the lowest fluxes. Hence, for the water fluxes, the study shows the following ranking of membrane supports independent of the permeating organic component:

Water : PEI > PVDF > PAN

In case of the organic fluxes two different trends were observed depending on the permeating component

Phenol : PVDF > PEI > PAN

Chloroform : PAN > PVDF > PEI

In order to explain the results it is necessary to take the geometric properties of the membrane support layer into account, see "Pervaporation Membranes." While the PVDF support has relative wide pores, the pores of the PAN support are very

Table 2. Fluxes, Permeabilties, and Selectivities of Phenol, Chloroform, and Water for Different PDMS Membranes

	PDMS–PVDF (5 μm)	PDMS–PVDF (1 μm)	PDMS–PAN (1 μm)	PDMS–PEI (1 μm)
Phenol flux [kmol/(m^2 hr)]	3.13×10^{-3}	5.04×10^{-3}	8.69×10^{-4}	4.41×10^{-3}
Water flux [kmol/(m^2 hr)]	6.67×10^{-2}	2.08×10^{-1}	6.94×10^{-2}	2.71×10^{-1}
Phenol permeability[a] [kmol/(m sec)]	3.88×10^{-11}	1.25×10^{-11}	2.12×10^{-12}	1.09×10^{-11}
Water permeability[a] [kmol/(m sec)]	1.15×10^{-10}	6.51×10^{-11}	2.00×10^{-11}	8.18×10^{-11}
Selectivity phenol [—]	12	6	3	4
Chloroform flux [kmol/(m^2 hr)]	1.97×10^{-3}	2.12×10^{-3}	2.50×10^{-3}	1.30×10^{-3}
Water flux [kmol/(m^2 hr)]	1.71×10^{-2}	3.30×10^{-2}	3.19×10^{-2}	4.79×10^{-2}
Chloroform permeability [kmol/(m sec)][a]	2.28×10^{-11}	4.88×10^{-12}	7.72×10^{-12}	2.07×10^{-12}
Water permeability[a] [kmol/(m sec)]	4.20×10^{-11}	1.31×10^{-11}	1.35×10^{-11}	1.57×10^{-11}
Selectivity chloroform [—]	298	158	158	65

[a] Using modified UNIFAC.

narrow. Therefore generally two phenomena can be considered to influence the mass transfer in case of the PAN-support and phenol:

1. pressure drop in the pores (see "Pressure Loss in the Support Layer"), and
2. pore condensation (see "Permeate Condensation in the Pores").

Both phenomena are directly related to the pore diameter and their potential significance in case of phenol can be further related to the fact that phenol with a low-equilibrium vapor pressure is more sensitive to changes of the permeate pressure than chloroform with a high-equilibrium vapor pressure. However, since the use of Eqs. (9)–(13) requires additional parameters of the support layer than those obtained, these explanations remain speculative. It seems though that in case of phenol the physical properties of the support layer are more important than the hydrophobicity of the support material. Hence, in the case of phenol the mass transfer is dominated by the physical properties of the membrane. In the case of chloroform, the hydrophobicity of the support material seems to mainly influence the chloroform fluxes.

Nevertheless, to ensure that the results from the fluxes were not influenced by other parameters, such as differences in membrane thickness, driving force, and concentration polarization, the permeabilities of the membranes were calculated according to the procedure described in "Estimation of the Permeability".

Apart from confirming the results taken from the analysis of the fluxes, another effect of the support layer on the mass transfer can be observed in Table 2. The permeabilities of the permeating components seem to increase significantly with membrane thickness. Using Eq. (3) the thickness of the interface layer of the PVDF-support is about 2.75 times larger than that of the PAN-support. Hence, it can be observed in accordance with theory ("Influence of Support Layer on the Diffusion Path") that the increase in diffusion path is more important for membranes with a thin selective layer than for membranes with a thick selective layer.

Studying the selectivities (see Table 2) regarding the influence of the different support layers, it can be observed that the selectivity is determined by permeabilities of the organic components. Hence, the support layer does not only influence the fluxes of the membrane but also the selectivity. The high selectivity of the PDMS–PVDF (5 μm) i.e., case of chloroform, can be related to its thicker selective layer compared to the other membranes.

From the different results it can be further seen that the systems with PEI-support can be classified according to Table 1 as Case III systems ($P_{w,support} \approx P_{w,M}$ and $P_{o,M} \gg P_{o,support}$) and described by Eqs. (9) and (20). The water flux in this system is higher compared to the other systems and in case of chloroform, when no additional effects, i.e., the physical properties of the support layer influence the flux, the organic flux is the lowest. Furthermore, compared to the PAN, which can be

Table 3. Fluxes, Permeabilities, and Selectivities of Different Aroma Components and Water Through POMS

Feed Components	POMS–PEI (5 μm)			POMS–PVDF (10 μm)		
	Flux [kmol/(m^2 hr)]	Permeability kmol/(m sec)][a]	Selectivity $\alpha_{o,W}$	Flux [kmol/(m^2 hr)]	Permeability [kmol/(m sec)][a]	Selectivity $\alpha_{o,w}$
Ethyl acetate	9.84×10^{-12}	5.22×10^{-5}	399	2.44×10^{-11}	6.48×10^{-5}	280
Ethyl butanoate	2.82×10^{-12}	1.43×10^{-4}	1445	7.57×10^{-12}	1.93×10^{-4}	1098
Ethyl-2-methyl butanoate	1.18×10^{-12}	1.58×10^{-4}	1785	2.90×10^{-12}	1.95×10^{-4}	1243
i-Butanol	2.96×10^{-12}	6.97×10^{-6}	45	7.17×10^{-12}	8.43×10^{-6}	31
i-Pentyl acetate (iso-amyl acetate)	1.73×10^{-12}	1.57×10^{-4}	1777	4.29×10^{-12}	1.95×10^{-4}	1244
Butanol	3.12×10^{-12}	7.35×10^{-6}	47	9.11×10^{-12}	1.07×10^{-5}	39
i-Pentanol (iso amyl alcohol)	2.15×10^{-12}	1.14×10^{-5}	87	5.87×10^{-12}	1.55×10^{-5}	67
t-2-Hexenal	5.65×10^{-12}	7.16×10^{-5}	610	1.71×10^{-11}	1.09×10^{-4}	522
Hexyl acetate	6.28×10^{-13}	1.49×10^{-4}	1867	1.46×10^{-12}	1.73×10^{-4}	1223
Hexanol	1.55×10^{-12}	2.04×10^{-5}	180	4.26×10^{-12}	2.79×10^{-5}	140
Water	3.70×10^{-12}	6.40×10^{-2}	—	1.31×10^{-11}	1.13×10^{-1}	—

[a] Using modified UNIFAC.

classified as a Case I/II system, the organic flux is about 1/3 lower. Assuming a porosity of 30% for all support materials, this would be in accordance with expectations. Both for the PAN-support and the PVDF support it is suggested to use Eqs. (17) and (18) proposed for Case II systems. To demonstrate that the findings regarding the support layer are not restricted to PDMS membranes, also (poly octylmethyl siloxane) (POMS) membranes tested by Börjesson et al. (l) were considered. The details of the experimental and analytical methods are given in Ref. (1). Assuming that the effect of concentration polarization and permeate pressure is negligible, the original results and the permeabilities determined according to "Estimation of the Permeability" are presented together with the selectivities in Table 3. The trends obtained are similar to those for the system chloroform–water with PDMS. Hence for the analyzed systems it can be assumed that the effects of the support layer are mainly related to the diffusion path, while the influence of pressure loss in the support layer and permeate condensation in the pores seem to be negligible. Overall, in accordance with the results for PDMS membranes, the POMS membrane with PEI support can be classified as a Case III membrane, see Table 1. The organic fluxes are generally lower than for the PVDF-supported POMS membrane, which can be described as a Case II membrane. Therefore, the theory proposed in this study seems to be applicable not only for composite membranes with a PDMS selective layer but also for composite membranes with other hydrophobic selective layers.

CONCLUSIONS

For the systems considered in this study it was observed that the support layer can have a significant impact on the fluxes and selectivities. The results indicate that the following guidelines to select an optimum support layer can be used.

1. The support layer material should be hydrophobic to improve the organic fluxes, and therefore the membrane selectivity.
2. The porosity of the support layer should be as high as possible to reduce the diffusion path through the membrane.
3. The pore diameters have to be optimized to avoid permeate condensation and permeate pressure loss on one hand and to reduce the length of the interface on the other hand. Special care has to be taken when optimizing the physical properties of the pores for components with a low-equilibrium vapor pressure, since the components are very sensitive to pore condensation and permeate pressure losses.
4. The effect of the interface layer and the increase in diffusion path have to be considered, particularly when thin selective lengths are produced. In these cases the pore diameters have to be optimized and the porosity maximized.

The above guidelines seem to be applicable for all membranes with a hydrophobic selective layer, and combined with the theory given in "Modeling of the Support layer in Hydrophobic Pervaporation", they should be used as a foundation to select support materials for improved composite membranes. One of the problems in this study was that the support layer data provided did not allow a detailed analysis of all phenomena influencing the mass transfer. Nevertheless, this study clearly revealed that the selection of the support structure could play a significant role in hydrophobic pervaporation. Since permeability and selectivity are both influenced by the support layer, selection of the appropriate support can have a significant influence of the performance and consequently the acceptance of hydrophobic pervaporation. Further investigations combining knowledge of material science, manufacturing processes, and modeling are required to gain further understanding on the influence of the support layer.

LIST OF SYMBOLS

A	area (m^2)
a	activity
d	diameter (m)
Kn	Knudsen number
k	mass transfer coefficient (m/sec)
l	length, thickness (m)
$\bar{l}$	average thickness (m)
M	molecular weight (kg/kmol)
J	solute flux [kmol/(m^2 sec)]
P	phenomenological permeability parameter [kmol/(m s)]
p	pressure (Pa, bar)
$\mathscr{R}$	resistance [(m^2 s)/kmol]
R	gas constant [J/(mol K)]
T	temperature (K)
$\tilde{V}$	molar volume (m^3/mol)
X	liquid phase molar fraction (mol/mol)
Y	vapor phase molar fraction (mol/mol)

Greek Letters

ϵ	membrane porosity
ϵ_S	surface porosity, defined in Eqs. (3) and (15)
γ	activity coefficient
η	dynamic viscosity (Pa s)
φ	fugacity coefficient
λ	mean free path, defined in Eq. (14) (m)

ρ_m	molar density (kmol/m^3)
σ	surface tension (N/m^2)
τ	tortuosity

Subscripts

Bo	boundary layer
F	feed
I	component *i*
Inter	interface layer
M	membrane
O	organic component
P	permeate
Path I	path I referring Fig. 1
Path II	path II referring Fig. 1
Pore	pore
Support	support layer
Total	total
W	water

Superscripts

Av	average
C	condensation
Sat	saturated

ACKNOWLEDGMENTS

The membranes used in the study were kindly provided by GKSS Forschungszentrum, Geesthacht (Germany). Further, F. Lipnizki wishes to acknowledge the financial support by a Druvan scholarship from the Dr. P. Håkanssons Foundation.

REFERENCES

1. Börjesson, J.; Karlsson, H.O.E.; Trägårdh, G. Pervaporation of a Model Apple Juice Aroma Solution: Comparison of Membrane Performance. J. Membr. Sci. **1996**, *119*, 229–239.
2. Franke, M. Auslegung und Optimierung von Pervaporationsanlagen zur Entwässerung und Lösungsmitteln. Ph.D. Thesis, University of Aachen, Germany.
3. Koops, G.H. Dehydration of Acetic Acid by Pervaporation; Material Science Aspects. Ph.D. Thesis, University of Twente, The Netherlands.

4. Burslem, R.H.; Naylor, T.deV.; Field, R.W. The Performance and Stability of Polyacrylate Membranes. In *Proceedings of the sixth International Conference in Pervaporation Processes in the Chemical Industry*; Bakish, R., Ed.; Bakish Material Corp.: Engelwood, NJ, 1992; 17–34.
5. Klatt, S. *Zum Einsatz von Pervaporation im Umfeld der chemischen Industrie*; Verlag Shaker: Aachen, 1993.
6. Heintz, A.; Stephan, W. A Generalized Solution-Diffusion Model of the Pervaporation Process Through Composite Membranes. Part II. Concentration Polarization, Coupled Diffusion and the Influence of the Porous Support Layer. J. Membr. Sci. **1994**, *89*, 153–169.
7. Bode, E.; Hoempler, C. Transport Resistance During Pervaporation Through a Composite Membrane: Experiments and Model Calculations. J. Membr. Sci. **1996**, *113*, 43–56.
8. Burslem, R.H. The Pervaporative Dewatering of Alcohol Using Caesium Polyacrylate Membranes. Ph.D. Thesis, University of Bath, UK.
9. Field, R.W.; Wu, P. The Choice of Support Layer of Polyacrylate Membranes for the Dehydration of Isopropanol by Pervaporation. *Int. Congr. Membr. Membr. Process. ICOM'96*, 1996; 398–399.
10. Nijhuis, H.H. Removal of Organics from Water by Pervaporation. Ph.D. Thesis, University of Twente, The Netherlands.
11. Stürken, K. Organophile Pervaporation: Ein Membranverfahren zur Aufarbeitung verdünnter wäßriger Lösungen. Ph.D. Thesis, University of Hamburg, Germany.
12. Scholz, H.; Hübner, A.; Kohnen, W.; Steinhauser, H.; Ellinghorst, G. Radiation Cured Composite Membranes: Optimum Combination of Selective Layer and Porous Support. In *Proceedings of the Fourth International Conference, Pervaporation Processes in the Chemical Industry*; Bakish, R., Ed.; Bakish Material Corp.: Engelwood, NJ, 1989; 189–198.
13. Heinzelmann, W. Fabrication Methods for Pervaporation Membranes. In *Proceedings of the Fifth International Conference, Pervaporation Processes in the Chemical Industry*; Bakish, R., Ed.; Bakish Material Corp.: Engelwood, NJ, 1991; 22–30.
14. Rautenbach, R.; Klatt, S. Treatment of Phenol-Contaminated Wastewater by a RO-PV Hybrid Process. In *Proceedings of the Fifth International Conference, Pervaporation Processes in the Chemical Industry*; Bakish, R., Ed.; Bakish Material Corp.: Engelwood, NJ, 1991; 392–408.
15. Borges, C.P.; Mulder, M.H.V.; Smolders, C.A. Composite Hollow Fiber for Removal of VOCs from Water by Pervaporation. In *Proceedings of the sixth International Conference, Pervaporation Processes in the Chemical Industry*; Bakish, R., Ed.; Bakish Material Corp.: Engelwood, NJ, 1992; 207–222.

16. Feng, X.; Huang, R.Y.M. Separation of Isopropanol from Water by Pervaporation Using Silicone-Based Membranes. J. Membr. Sci. **1992**, *74*, 171–181.
17. Vankelecom, I.F.J.; Moersmans, B.; Verschueren, G.; Jacobs, P.A. Intrusion of PDMS Top Layers in Porous Supports. J. Membr. Sci. **1999**, *158*, 289–297.
18. Henis, J.M.S.; Tripodi, M.K. A Novel Approach to Gas Separation Using Composite Hollow Fiber Membranes. Sep. Sci. Technol. **1980**, *15*, 1059–1068.
19. Henis, J.M.S.; Tripodi, M.K. Composite Hollow Fiber Membranes for Gas Separation: The Resistance Model Approach. J. Membr. Sci. **1981**, *8*, 233–246.
20. Nakagawa, T. Gas Separation and Pervaporation. In *Membrane science and technology*; Osada, Y., Nakagawa, T., Eds.; Marcel Dekker: New York, 1992; 239–287.
21. Gudernatsch, W.N. Integration des Pervaporativen Produktaustrags in die Fermentation von Organischen Lösungsmitteln. Ph.D Thesis, University of Stuttgart, Germany.
22. Gudernatsch, W.N.; Menzel, T.; Strathmann, H. Influence of Composite Membrane Structure on Pervaporation. J. Membr. Sci. **1991**, *61*, 19–30.
23. Bai, J.; Fouda, E.; Matsuura, T.; Hazlett, J.D. A Study on the Preparation and Performance of Polydimethylsiloxane-Coated Polyetherimide Membranes in Pervaporation. J. Appl. Polym. Sci. **1993**, *48*, 999–1008.
24. Gekas, V.; Trägårdh, G.; Hallström, B. *Ultrafiltration Membrane Performance Fundamentals; 10 Years of Characterization and Fouling Studies*; ISBN-91-630-2231-1, Department of Food Engineering: Lund University, Sweden, 1993.
25. Brodkey, R.S.; Hershey, H.C. *Transport Phenomena. Unified Approach*; McGraw-Hill Book Company: New York, 1988.
26. Mulder, M.H.V. *Basic Principles of Membrane Technology*; Kluwer Academic Publishers: Dordrecht, The Netherlands, 1991.
27. Beuscher, U.; Gooding, C.H. The permeation of Binary Gas Mixtures Through Support Structures of Composite Membranes. J. Membr. Sci. **1998**, *150*, 57–73.
28. Albrecht, R. Pervaporation—Beiträge zur Verfahrensentwicklung. Ph.D. Thesis, University of Aachen, Germany.
29. Rautenbach, R.; Albrecht, R. On the Behaviour of Asymmetric Membranes in Pervaporation. J. Membr. Sci. **1984**, *19*, 1–22.
30. Karlsson, H.O.E.; Trägårdh, G. Pervaporation of Dilute Organic–Water Mixtures. A Literature Review on Modeling Studies and Applications to Aroma Recovery. J. Membr. Sci. **1993**, *76*, 121–146.

31. Lipnizki, F.; Hausmanns, S.; Ten, P.K.; Field, R.W.; Laufenberg, G. Organophilic Pervaporation: Prospects and Performance. Chem. Eng. J. **1999**, *73*, 113–129.
32. Bennett, M. Pervaporation Using Modified Polysiloxanes: Removal of Organic Contaminants from Aqueous Streams. Ph.D. Thesis, University of Bath, UK.
33. Smith, K.A.; Colton, C.K.; Merrill, E.W.; Evans, L.B. Convective Transport in a Batch Dialyzer: Determination of True Membrane Permeability from a Single Measurement. Chem. Eng. Prog. Sym. Ser. **1968**, *64* (No. 84), 45–58.
34. Reid, R.C.; Prausnitz, J.M.; Poling, B.E. *The Properties of Gases and Liquids*, 4th Ed.; McGraw-Hill: New York, 1987.

Received February 2001
Revised September 2001